THE UNIVERSITY OF MICHIGAN

INDUSTRY PROGRAM OF THE COLLEGE OF ENGINEERING

RESONANCE IN LIQUID ROCKET ENGINE SYSTEMS

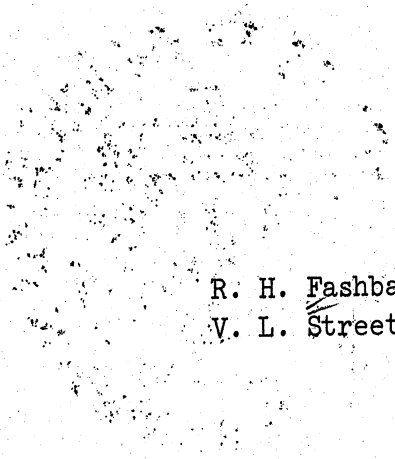

R. H. Fashbaugh
V. L. Streeter

April, 1965

IP-698

TABLE OF CONTENTS

	Page
LIST OF FIGURES	v
INTRODUCTION	1
THE ROCKET ENGINE PROPELLANT SYSTEM	3
FLUID TRANSIENT EQUATIONS	7
PIPE END BOUNDARY EQUATIONS	10
1. Upstream End of Pipe 1	10
2. Junction of Pipe 1 and Pipe 2	10
3. Junction of Pipes 4, 5, and 6	11
4. Pulser Boundary Condition	12
5. Downstream End of Pipe 7	12
TURBOPUMP REPRESENTATION	14
THE COMPUTER PROGRAM	19
RESULTS OF THE ANALYSIS	22
COMBINING THE PROPELLANT SYSTEMS WITH THE SUPPORTING STRUCTURE	27
CONCLUSIONS	29
APPENDIX A	30
REFERENCES	32

LIST OF FIGURES

Figure		Page
1	Missile Rocket Engine Feed System	4
2	Oxidizer Feed System Test Configuration	5
3	Oxidizer Pump Steady State Characteristic Curves	6
4	Method of Characteristics Mesh	8
5a	Computer Flow Diagram	20
5b	Computer Flow Diagram Continued	21
6	Oxidizer Pump Transient Suction Pressure Versus Frequency	23
7	Oxidizer Pump Transient Pressure Ratio and Discharge system Transient Pressure Ratio versus Frequency	24
8	Fuel Pump Transient Suction Pressure versus Frequency	25
9	Fuel Pump Transient Pressure Ratio and Discharge System Transient Pressure Ratio versus Frequency	26
10	Diagram of Combined Propellant System, Engine, and Structure Analysis	28

INTRODUCTION

A development problem associated with the Titan II missile was a self-exited longitudinal vibration set up in the missile structure and the rocket engine propellant feed system. At one condition of operation a structure resonance developed which was reinforced by propellant system resonances. The motion of the feed tank and pump caused the outflow to the thrust chamber and the resultant thrust, to vary periodically at the natural frequency of the structural assembly.

This analysis deals primarily with the transients in all the pipes of the engine feed system and especially focuses on the method of representing the turbopump transient characteristics analytically, including the effect of pump inlet impeller cavitation. The quasi-linear partial differential equations of continuity and momentum were solved by the methods of characteristics and the method of specified time intervals, and by use of finite difference methods placed in convenient form for use with a large digital computer. Non-linear friction losses in piping were included, and the turbopump transient pressure rise is included as a non-linear function of the transient flow rate and inlet pump static pressure.

The propellant system analyzed is a full-scale ground test simulation of the missile propellant system. These results were compared with the actual ground tests which included the turbopumps and feed system. In these tests (and in the analytical representation) the engine feed system was hydraulically the same as the

actual missile system except that the engine fuel and oxidizer injectors were simulated by orifices and the engine thrust chamber and nozzle were similated by a cavitating venturi. The fuel and oxidizer systems were tested separately.

THE ROCKET ENGINE PROPELLANT SYSTEM

A sketch of the rocket engine propellant system is shown in Figure 1. Both the fuel and oxidizer systems include a propellant tank, a line from the tank to the turbopump inlet, the turbopump and a line from the turbopump discharge to the thrust chamber injector. Valves are located upstream of each pump and injector.

A sketch of the oxidizer system ground test configuration which simulates the missile system is shown in Figure 2. The fuel system test simulation was similar. The hydraulic dynamic resistance for the cavitating venturi is twice that of the hydraulic dynamic resistance for the engine nozzle. This fact was taken into account when the test data were evaluated for the missile application, but is of no concern to this treatment since the analysis is of the test configuration.

The fuel and oxidizer turbopump characteristic curves are shown in Figure 3. Since this is a dynamic problem, interest is primarily in the slope of these curves at a particular operating point, such as shown on the curves. The use of these curves as well as other parameters such as friction factors and pressure wave velocities, orifice and venturi coefficients are discussed subsequently.

The fuel and oxidizer used in the test were the same as the missile propellants which are Aerogine 50 (50% Hydrazine, 50% UDMH) and nitrogen tetroxide.

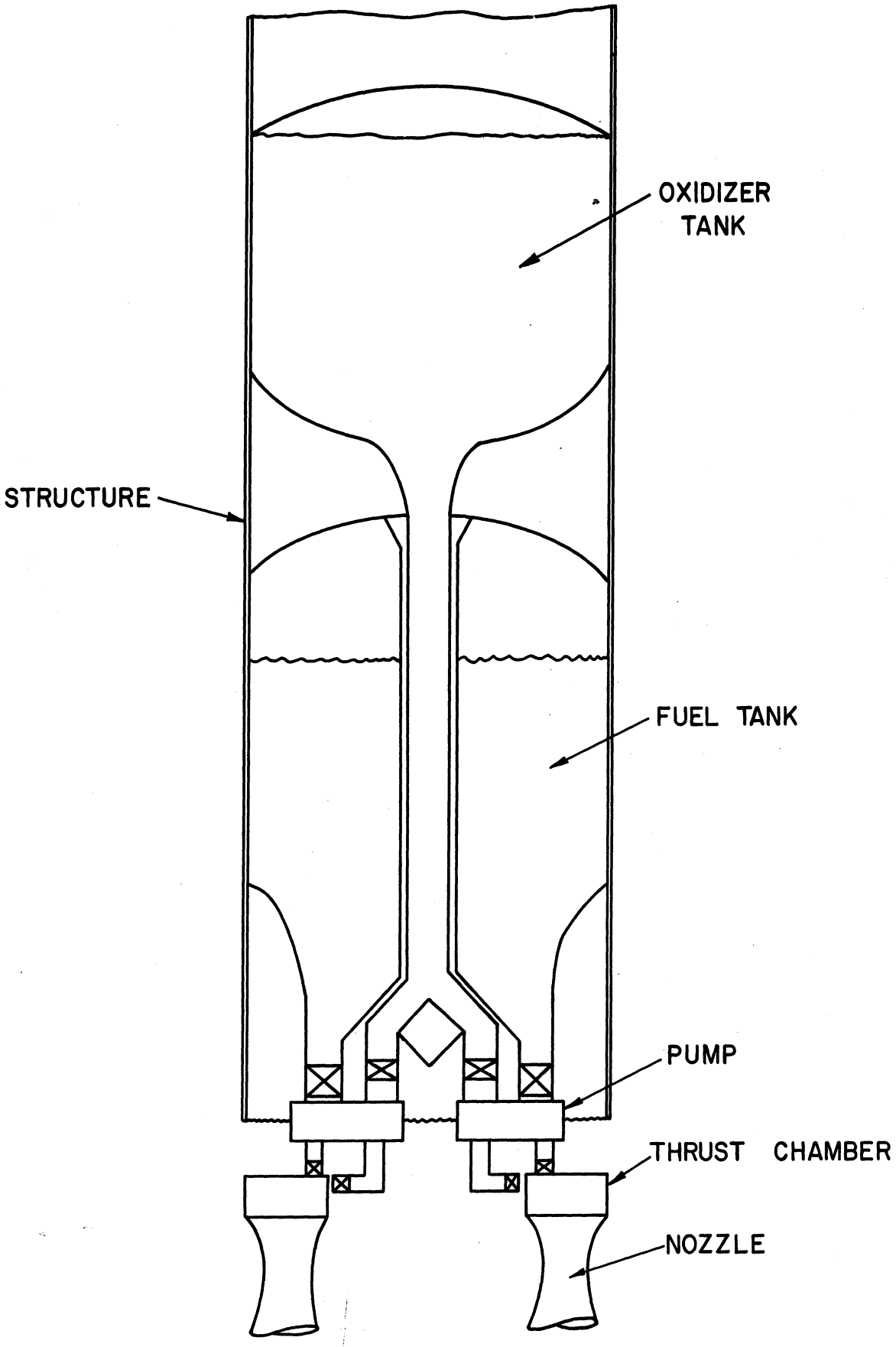

Figure 1. Missile Rocket Engine Feed System.

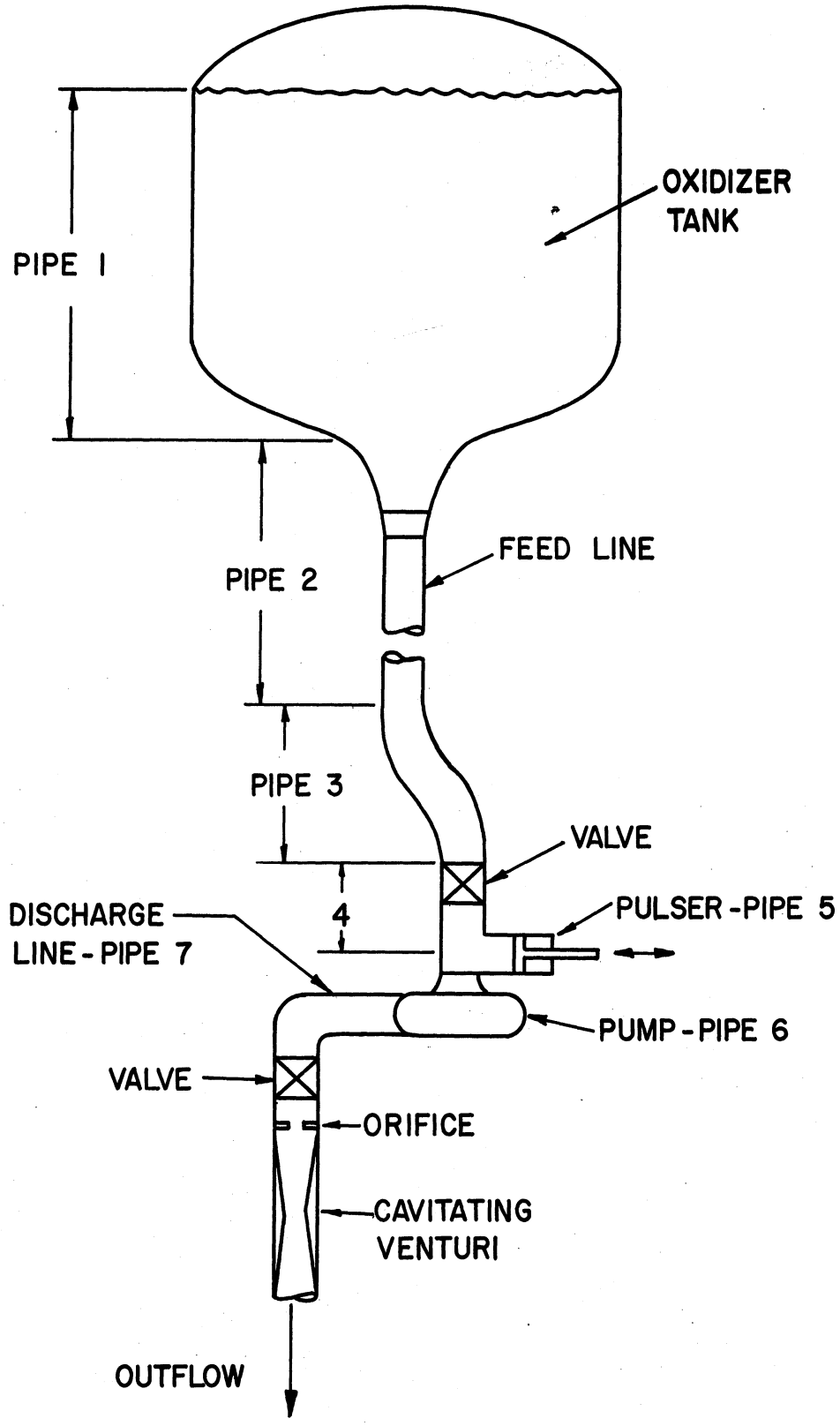

Figure 2. Oxidizer Feed System Test Configuration.

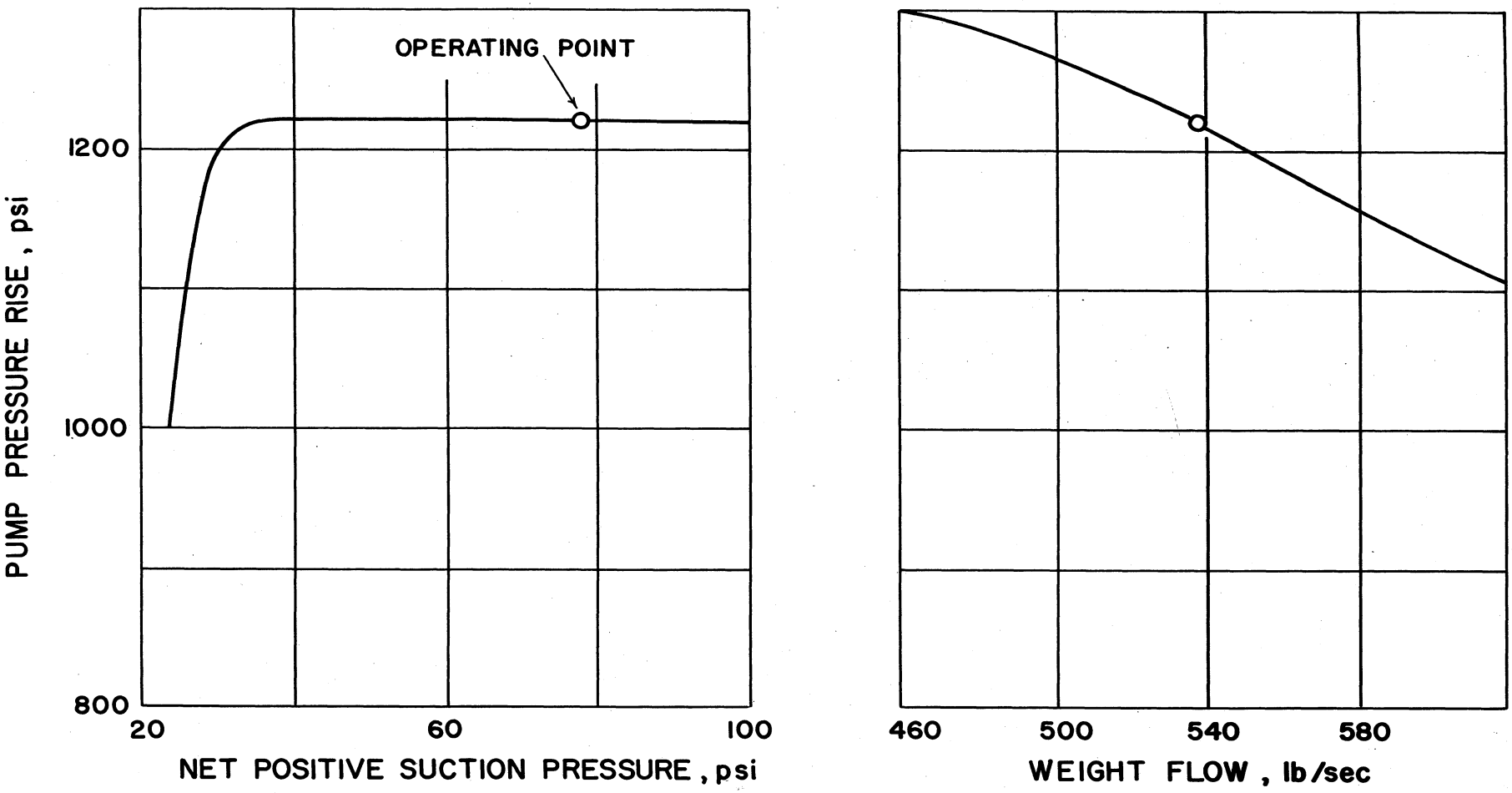

Figure 3. Oxidizer Pump Steady State Characteristics.

FLUID TRANSIENT EQUATIONS

The methods of calculating head and velocity of small time intervals for equally-spaced sections along a pipeline, with inclusion of friction, have been previously reported.[1,2,3] The important working equations are briefly summarized:

For the interior sections along a pipe

$$V_p = \frac{1}{2}\left[V_R + V_S + g(H_R - H_S)/a_C - (fV^2)_C\,\Delta t/D\right] \qquad (1)$$

and

$$H_p = \frac{1}{2}\left[H_p + H_S + a_C\,(V_R - V_S)/g\right] \qquad (2)$$

in which V_p and H_p are velocity and elevation of a hydraulic grade-line at section P. With reference to Figure 4, it is considered that V and H at A, C, and B have previously been calculated. V_R, V_S, H_R and H_S are obtained by linear interpolation between A, C, and B by the formulas

$$V_R = V_C + \theta(V + a)_C\,(V_A - V_C) \qquad (3)$$

$$H_R = H_C + \theta(V + a)_C\,(H_A - H_C) \qquad (4)$$

$$V_S = V_C + \theta(V - a)_C\,(V_C - V_B) \qquad (5)$$

$$H_S = H_C + \theta(V - a)_C\,(H_C - H_B) \qquad (6)$$

in which $\theta = \Delta t/\Delta X$, the preselected mesh ratio for the calculations. C^+ and C^- of Figure 4 are the characteristics. For the method to be stable, it is essential that

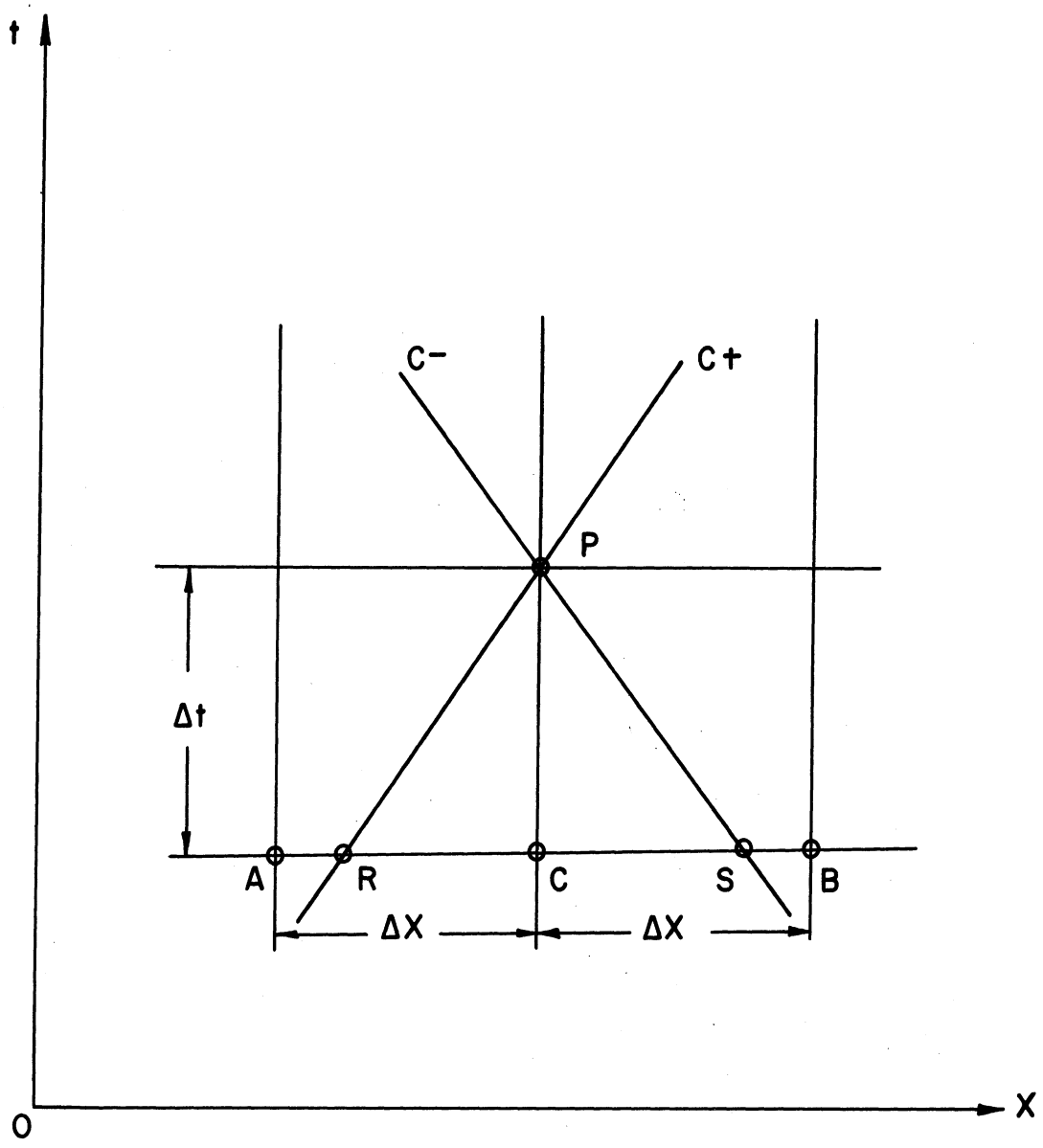

Figure 4. Characteristic Curves.

$$\theta < \frac{1}{|V| + a} \tag{7}$$

in which 'a' is the speed of a pressure pulse wave.

$$a = \left[\frac{K}{\rho(1 + \frac{KD}{Eb})} \right]^{1/2} \tag{8}$$

K is the bulk modulus of elasticity of the fluid, ρ the mass density, E the Young's modulus for pipe wall material, D the pipe diameter, and b the wall thickness. In the equations, g is the acceleration of gravity, f the Darcy-Weisbach friction factor, and Δt the time increment used in the calculations. The subscript C denotes evaluation of the quanity at the section under consideration for the preceding time increment.

At the end sections of a pipe, the characteristic equations yield one equation in the two unknowns V_p and H_p. For the downstream end

$$V_p = V_R - g(H_p - H_R)/a_C - \frac{1}{2} \Delta t (fV^2)_C / D \tag{8}$$

and for the upstream end

$$V_p = V_S + g(H_p - H_S)/a_C - \frac{1}{2} \Delta t (fV^2)_C / D \tag{9}$$

External conditions (pipe end boundary conditions) must supply the extra relationship so that V_p and H_p may be calculated.

PIPE END BOUNDARY EQUATIONS

The pipe external or end boundary equations will be given for the oxidizer system pipes. The boundary equations for the fuel system pipes are derived in a similar manner.

As shown in Figure 2 the oxidizer system test configuration was represented by 7 pipes; 1 pipe for the tank, 3 pipes for the pump feed line, 1 pipe to represent the pump, 1 pipe for the pump discharge line and 1 pipe to represent the pulser. Each pipe was divided into sections as previously explained. The boundary equations for the end of each pipe in the system are as follows:

1. Upstream End of Pipe 1

The pressure head at the inlet to pipe 1 is

$$H_p(1,1) = H_g \tag{10}$$

where H_g is the gas pressure head in the tank and $H_p(1,1)$ is the pressure head in pipe 1 of section 1.

2. Junction of Pipe 1 and Pipe 2

The pressure head at the downstream end of pipe 1 (tank outlet) is equal to the pressure head at the upstream end of pipe 2, so that

$$H_p(1,N1) = H_p(2,1) \tag{11}$$

where $H_p(1,N1)$ indicates the pressure head in pipe 1, section N (the last section) and $H_p(2,1)$ indicates the pressure head in pipe 2,

section 1 . This notation will be used throughout the text. Another relation is derived from continuity of flow from pipe 1 to pipe 2 as

$$V_p(1,N1) = \left(\frac{D_2}{D_1}\right)^2 V_p(2,1) \qquad (12)$$

where D_1 and D_2 are the diameters of pipes 1 and 2 respectively.

The above two equations along with the two boundary characteristic equations previously derived (one for each pipe) give the required four equations to solve for the four unknowns, $H_p(1,N1)$, $V_p(1,N1)$, $H_p(2,1)$, and $V_p(2,1)$.

The boundary equations for pipe junctions 2 to 3, 3 to 4, and 6 to 7 are identical to the equations for junction 1 to 2 except for the subscripts.

3. Junction of Pipes 4, 5, and 6

As in the junction of pipes 1 and 2 , the pressure head is equal, so that

$$H_p(5,1) = H_p(4,N4) \qquad (13)$$

$$H_p(6,1) = H_p(4,N4) \qquad (14)$$

From continuity we have,

$$V_p(4,N4) = \left(\frac{D_5}{D_4}\right)^2 V_p(5,1) + \left(\frac{D_6}{D_4}\right)^2 V_p(6,1) \qquad (15)$$

These three equations along with three characteristic equations (one for each pipe) determine the six unknowns, $H_p(4,N4)$, $V_p(4,N4)$, $H_p(5,1)$, $V_p(5,1)$, $H_p(6,1)$, and $V_p(6,1)$.

4. Pulser Boundary Condition

There are two unknowns at the pulser piston, $H_p(5,N5)$ and $V_p(5,N5)$. One characteristic equation is available and the other necessary equation is simply

$$V_p(5,N5) = L_o \omega \sin \omega t \tag{16}$$

where L_o is the pulser stroke and ω is the angular frequency. The pulser inputs a sinusoidal variation in flow to the system.

5. Downstream End of Pipe 7

Since pipe 7 is terminated in an orifice the orifice equation is used to determine the boundary condition equation. If H_o is the pressure head downstream of the orifice and D_7 and D_o are pipe 7 and orifice diameters respectively,

$$V_p(7,N7)\left(\frac{\pi}{4}D_7^2\right) = C_{DO}\left(\frac{\pi}{4}D_o\right)^2 \left[2g(H_p(7,N7) - H_o)\right]^{1/2} \tag{17}$$

$$V_p(7,N7) = C_{DO}\left(\frac{D_o}{D_7}\right)^2 \left[2g(H_p(7,N7) - H_o)\right]^{1/2} \tag{18}$$

Since the pressure at the throat of the cavitating venturi is vapor pressure the pressure head, H_o, can be determined from

$$V_p(7,N7) = C_{DV}\left(\frac{D_V}{D_7}\right)^2 \left[2g(H_o - H_V)\right]^{1/2} \tag{19}$$

$$H_o = \frac{1}{2g}\left(V_p(7,N7)\right)^2 \left(\frac{D_7^2}{C_{DV}D_V^2}\right)^2 + H_V \tag{20}$$

Equations (18) and (20) yield the desired boundary equation

$$V_p(7,N7) = C_{DO}\left(\frac{D_o}{D_7}\right)^2 \left[\frac{2g(H_p(7,N7) - H_V)}{1 + \left(\frac{C_{DO}}{C_{DV}}\right)^2 \left(\frac{D_o}{D_V}\right)^4}\right]^{1/2} \qquad (21)$$

where C_{DO} and C_{DV} are orifice and cavitating venturi discharge coefficients, D_V is the venturi throat diameter and H_V is the vapor pressure of the propellant in feet of head.

TURBOPUMP REPRESENTATION

Referring to characteristic Equation (1), the friction term can be written

$$\frac{1}{2}(fV^2)_C \, \Delta t/D = g\left(\frac{\Delta H}{\Delta X}\right)\Delta t \qquad (22)$$

where ΔH is the pressure head drop in the distance ΔX. Since internal losses in a pump are reflected in the pump head rise the friction term should not appear in the pump (pipe 6) equations. Instead, it is readily seen from Equation (22) that the term

$$g\left(\frac{\Delta H_p}{L_p}\right)\Delta t \qquad (23)$$

can be substituted for the friction term in the pipe 6 equations but with opposite sign to represent the pump head rise. L_p is the length of the pump flow path and ΔH_p is the pump head rise. The characteristic equation for pipe 6 corresponding to Equation (1) is then

$$V_p = \frac{1}{2}\left[(V_R + V_S) + g(H_R - H_S)/a_C + 2g\left(\frac{\Delta H_p}{L_p}\right)\Delta t\right] \qquad (24)$$

Equations (2) through (6) do not change because of the pump head rise and will apply to pipe 6.

The steady state pump head rise is a function of both the pump inlet pressure and flowrate as is shown on Figure 3. It was assumed that for transient conditions the head rise could be determined from these steady state characteristic curves. It was also assumed that affects due to variations in the pump speed were negligible.

Equations for the characteristic curves (Figure 3), determined by curve fitting methods, were used to compute the head rise, ΔH_p, for particular values of inlet pressure and flowrate. The equation for ΔH_p is

$$\Delta H_p = \Delta H_{po} - B_0(V_p(6,1) - V_o)^2 - \left(B_1 - \frac{(H_p(6,1) - H_{po})}{B_2 + B_3(H_p(6,1) - H_{po})}\right) \tag{25}$$

In this equation ΔH_{po}, B_0, and V_o are constants determined from the steady state head rise versus flowrate curve and H_{po}, B_1, B_2, and B_3 are constants determined from the steady state head rise versus inlet pressure curve.

The cavitation of the pump inlet impeller has a large effect on the fluid transients in the suction system. Tests at the Martin-Marietts Corporation (Denver Division) have shown that a region of cavitation can extend in the pump inlet pipe as far as from three to four feet upstream of the inlet to the oxidizer pump. This cavitation region drastically lowers the pressure-wave velocity in the inlet pipes and therefore lowers the quarter wave resonant frequency of the entire pump feed system. Since there is no way of computing the effect of this cavitation, the pressure wave velocity near the pump has to be approximated from test data. In this case, the quarter wave resonant frequency of each feed line used in the analysis was the value measured in the tests and pressure wave velocities for the feed system pipes were derived from

these measured values. It is also possible to determine these resonant frequencies from a spectrum analysis of pump inlet pressure measured during engine test firings.

The fuel pump feed pipe is short and it was assumed therefore that the cavitation affected the pressure wave velocity in the entire pipe. The length of pipe from the tank outlet to the pump inlet will be a quarter wave length. The average pressure wave velocity in the pipe is therefore

$$a_f = 4 f_{nf} L_f \tag{26}$$

where f_{nf} is the quarter wave resonant frequency and L_f is the length of the fuel pump feed pipe.

The oxidizer feed pipe is long and the cavitation will only affect a small portion of the pipe. The pipe was therefore considered as three pipes each with a different pressure wave velocity. In this case they are denoted pipe 2, 3, and 4. The pressure wave velocity in pipe 2 was computed using Equation (8), the pressure velocity in pipe 3 was taken as one half the value of pipe 2, and the pressure wave velocity in pipe 4 was determined so that the system resonant frequency would be equal to the measured value.

Since the friction loss is small, the impedance relations for a lossless fluid pipe were used to determine the pressure wave velocity in pipe 4. The surge impedance for pipe 2 is

$$Z_{o2} = \frac{a_2}{\frac{\pi}{4} D_2^2 g} \tag{27}$$

and the impedance of the downstream end of pipe 2, since the impedance of the tank end is very small, is

$$Z_2 = j Z_{o2} \tan \beta_2 L_2 \tag{28}$$

where

$$\beta_2 = \frac{2\pi f_{no}}{a_2} \tag{29}$$

and L_2 is the length of pipe 2 and f_{no} is the quarter wave resonant frequency. Similarly, the relations for pipes 3 and 4 are

$$Z_{o3} = \frac{a_3}{\frac{\pi}{4} D_3^2 g} \tag{30}$$

$$Z_3 = Z_{o3} \left[\frac{Z_2 + j Z_{o3} \tan \beta_3 L_3}{Z_{o3} + j Z_2 \tan \beta_3 L_3} \right] \tag{31}$$

$$\beta_3 = \frac{2\pi f_{no}}{a_3} \tag{32}$$

$$Z_{o4} = \frac{a_4}{\frac{\pi}{4} D} \tag{33}$$

$$Z_4 = Z_{o4} \left[\frac{Z_3 + j Z_{o4} \tan \beta_4 L_4}{Z_{o4} + j Z_3 \tan \beta_4 L_4} \right] \tag{34}$$

$$\beta_4 = \frac{2\pi f_{no}}{a_4} \tag{35}$$

Since Z_4 represents the impedance of the entire feed system at the pump inlet, this impedance will be maximum at the quarter wave resonant frequency f_n. Therefore, the denominator of Equation (34) will be zero at the frequency f_n which provides the expression from which the pressure wave velocity a_4 can be obtained.

$$Z_{o4} + j\, Z_3 \tan \beta_4 L_4 = 0 \tag{36}$$

Using the first two terms of the tangent series and the expressions for Z_4 and β_4 Equation (36) becomes

$$a_4^4 - \frac{1}{2} |Z_3| (\pi^2 D_4^2 g f_{no} L_f) a_4^2 - \frac{2}{3} |Z_3| (\pi^4 D_4^2 g f_{no}^3 L_4^3) = 0 \tag{37}$$

which yields

$$a_4 = \left\{ 2.46\, f_{no} L_4 D_4^2 g\, |Z_3| \left[1 + \sqrt{1 + \frac{10.7\, f_{no} L_4}{D_4^2 g\, |Z_3|}} \right] \right\}^{1/2} \tag{38}$$

This is an approximation for the effect of the cavitation. The most important aspect is that the pump feed lines in the analysis have the proper quarter wave resonant frequency.

THE COMPUTER PROGRAM

An abbreviated flow diagram for the solution of the fluid transients in the oxidizer system is illustrated in Figures 5a and 5b. The steady-state pressure heads, velocities, and the pressure wave velocity for each pipe are computed, stored, and printed for time $t = 0$. The velocity and pressure head for the interior sections of each pipe are computed from the same block of equations and the boundary points between the pipes are then computed from the boundary equations for time $t + \Delta t$. The time increment Δt is chosen so that the interpolation points R and S lie within points A and C of Figure 4. The computed values are printed and stored for the next computation. The result is a time history of pressure head and velocity at each section of each pipe in the system.

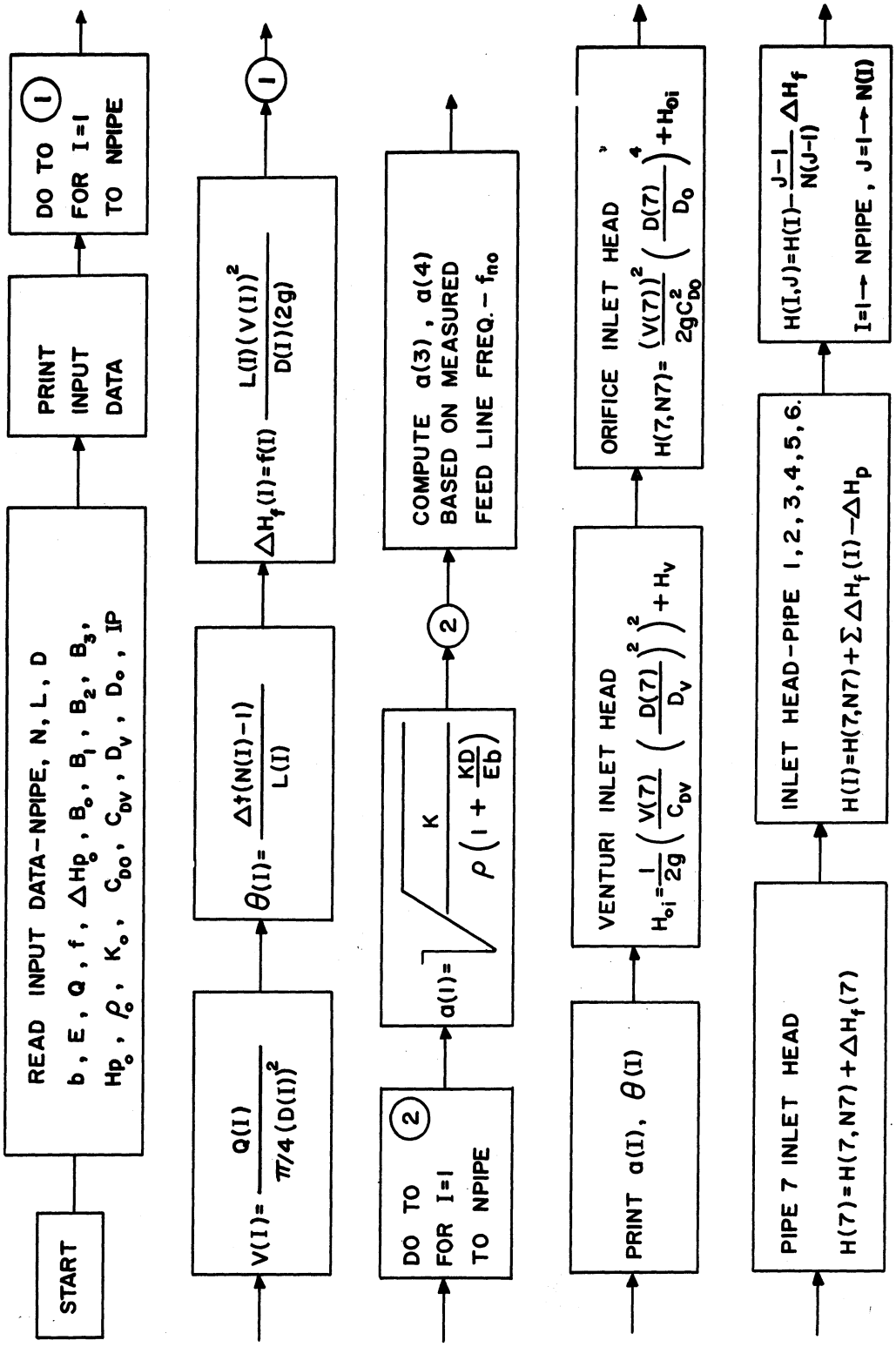

Figure 5a. Computer Flow Diagram.

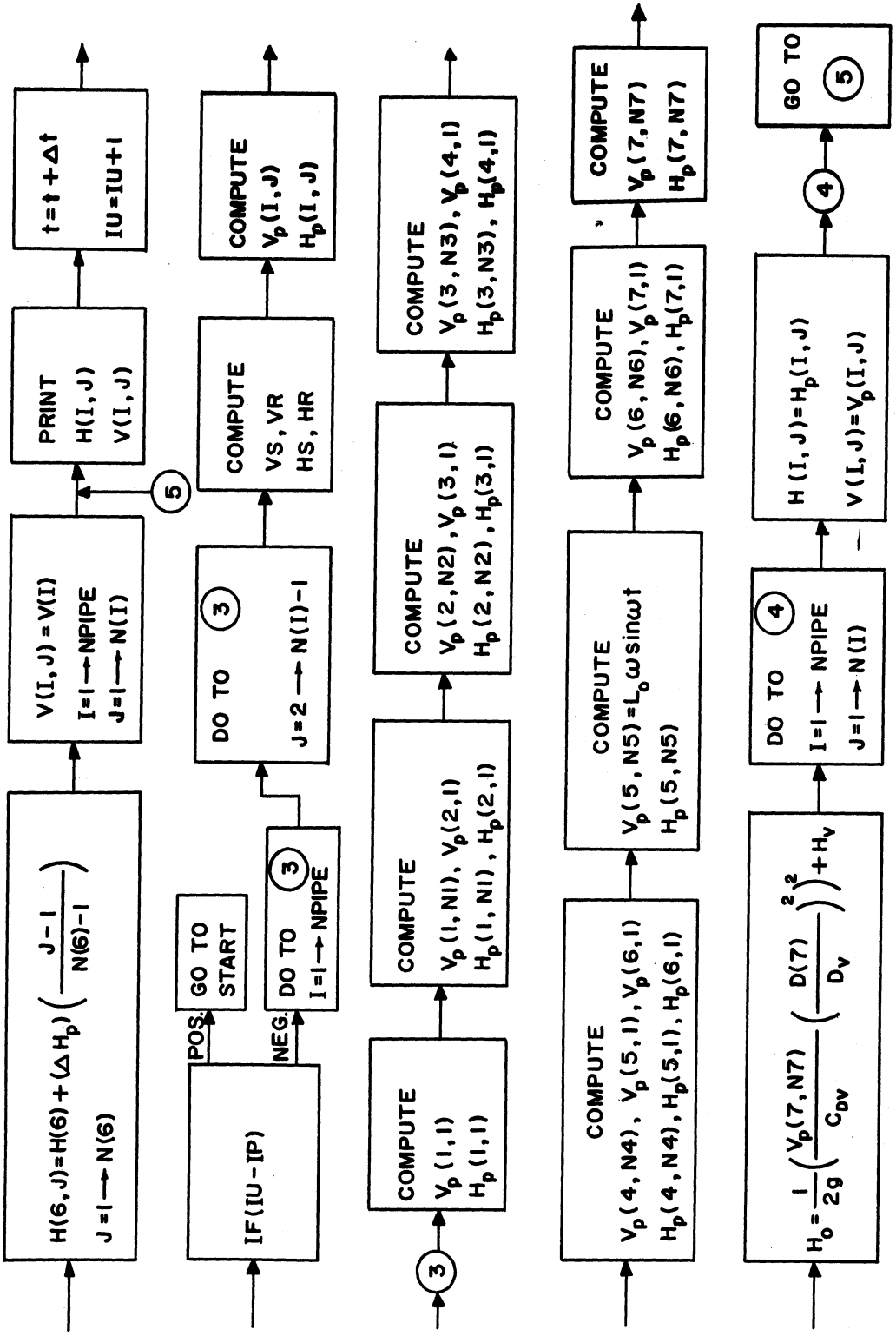

Figure 5b. Computer Flow Diagram (Continued).

RESULTS OF THE ANALYSIS

The results of the analysis compared with test results are shown in Figures 6 through 9. Figures 6 and 8 illustrate the ratio of the amplitude of the pump inlet pressure oscillation to the corrected acceleration amplitude of the pulser versus frequency. The pulser acceleration amplitude is corrected by the ratio of the flow area of the pulser to the flow area of the pump inlet pipe. These curves show a good agreement of the analysis results to test data.

Curves are shown in Figures 7 and 9 which compare the ratio of the amplitude of the pump discharge oscillation to the amplitude of the pump inlet oscillation. These ratios depend upon the pump dynamic characteristics. The agreement is fairly good which shows that the pump steady state characteristic curves are adequate for use in dynamic problems. The test data was quite non-linear for the fuel pump around the resonant frequency of 12 cps which could account for the deviation of the analysis results from the data around this frequency.

Curves are also shown in Figures 7 and 9 which compare the pump discharge pressure oscillation amplitude to the amplitude of the venturi inlet pressure oscillation. The analytical results compare well with the data which substantiates the analytical representation of the pump discharge systems.

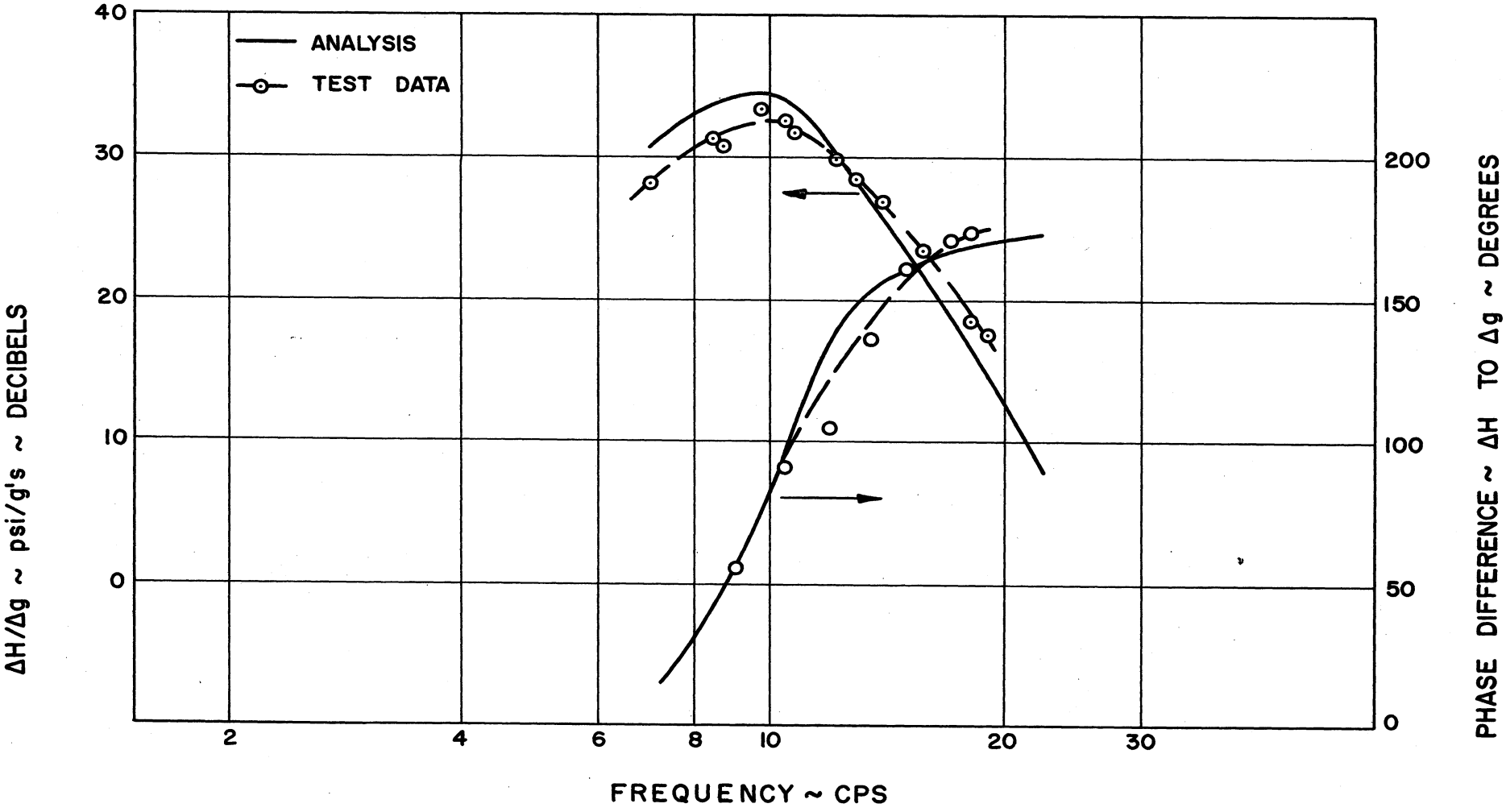

Figure 6. Oxidizer Pump Transient Suction Pressure.

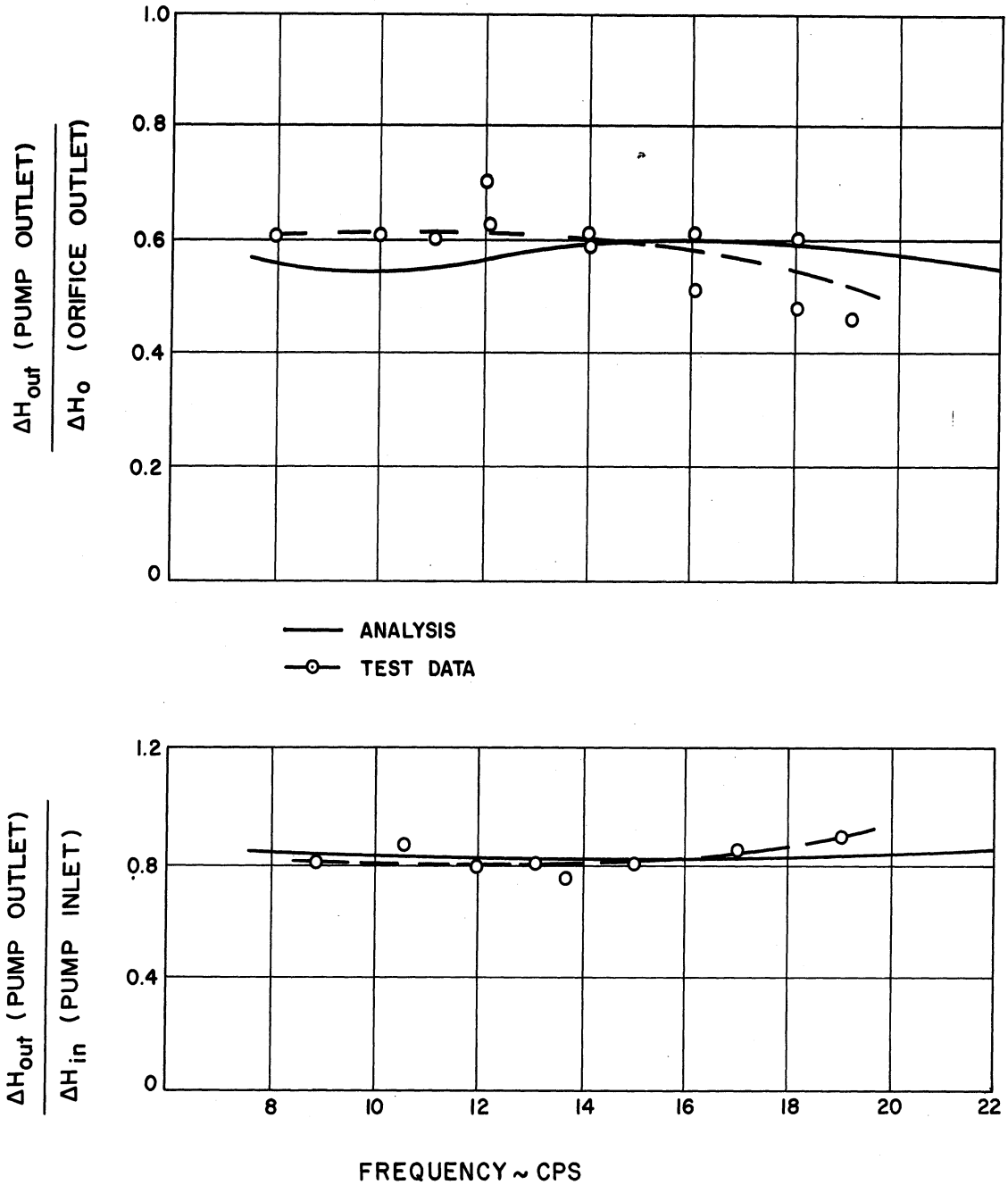

Figure 7. Oxidizer Pump Pressure Ratio and Discharge System Pressure Ratio.

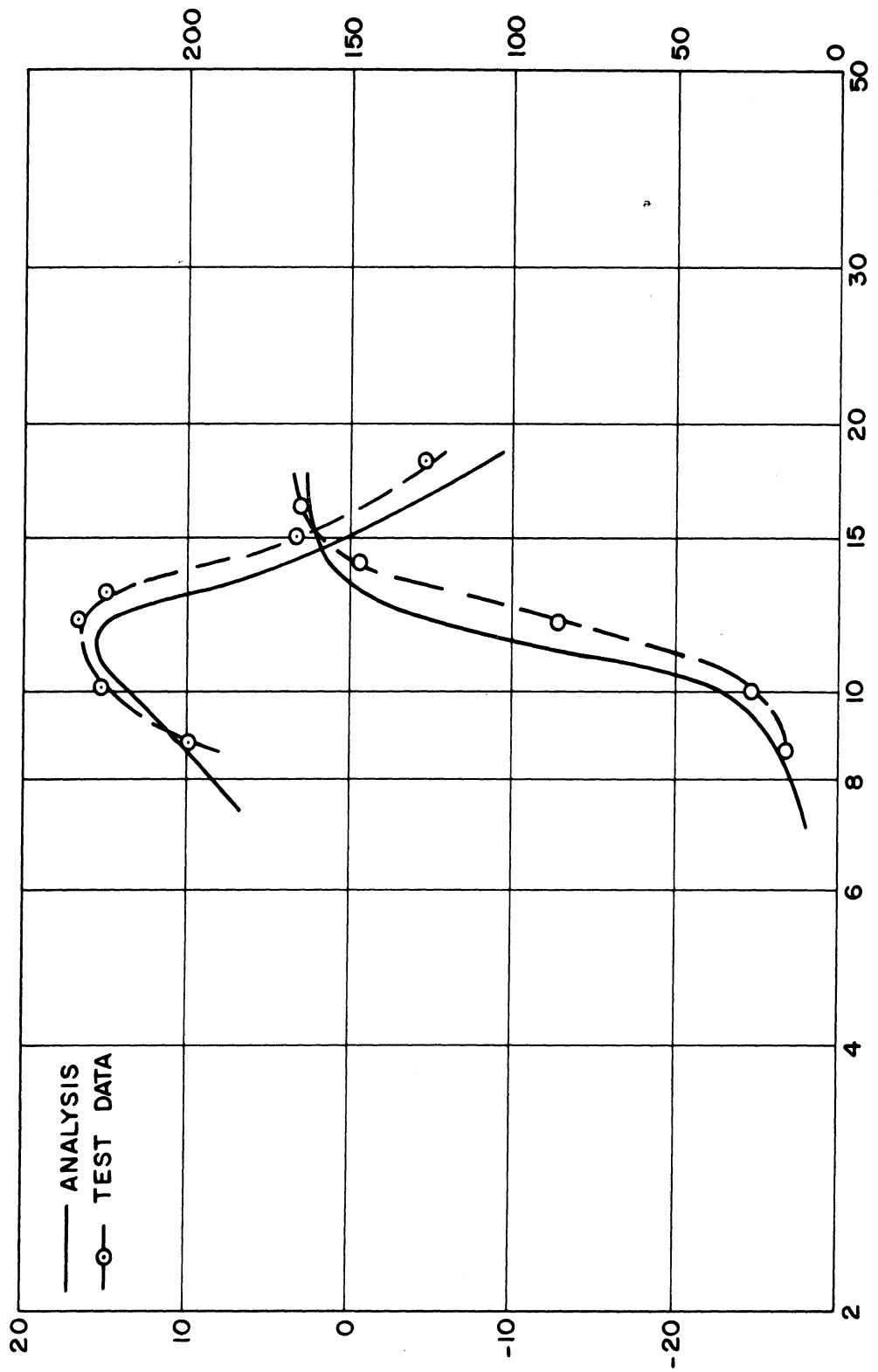

Figure 8. Fuel Pump Transient Suction Pressure.

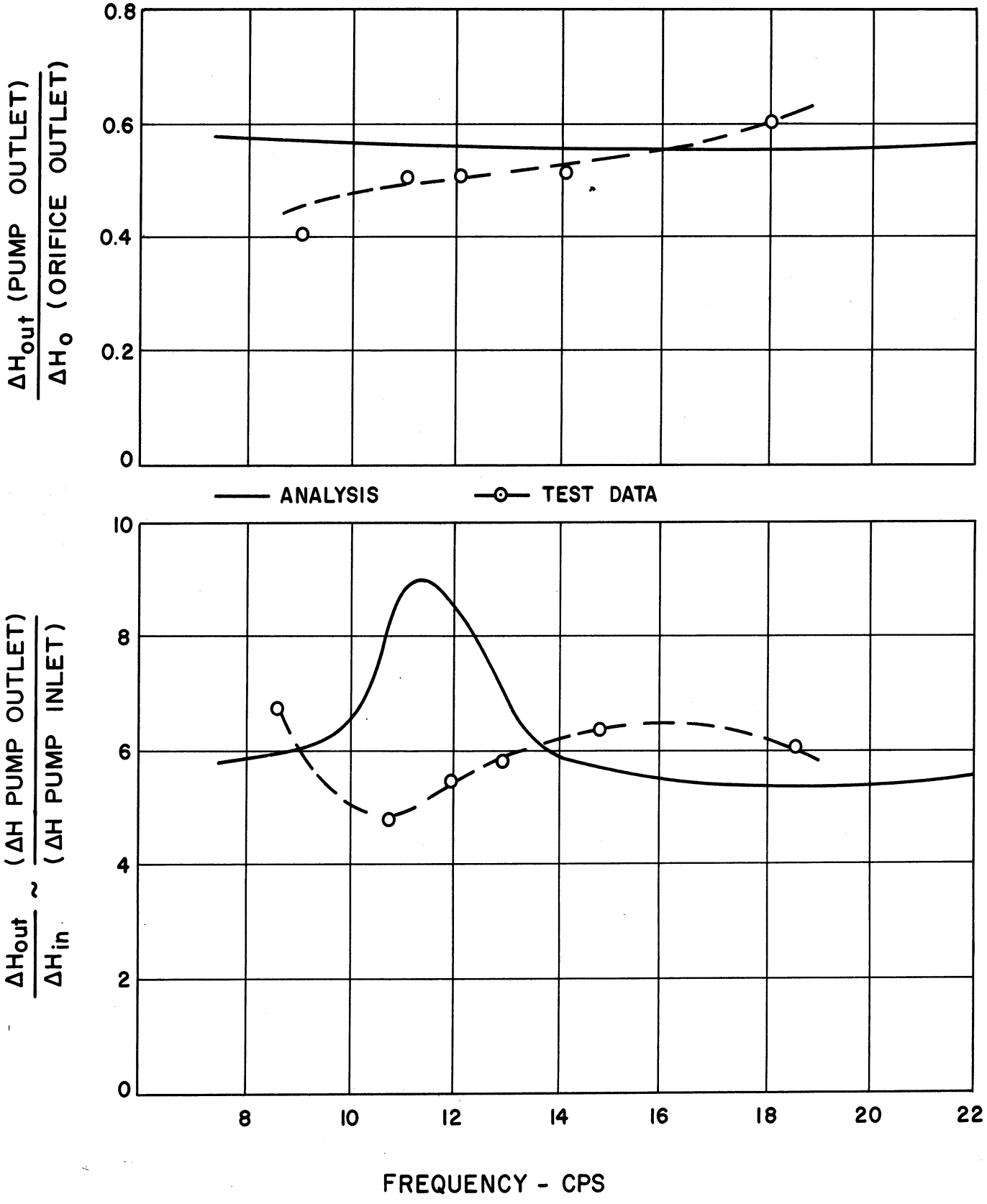

Figure 9. Fuel Pump Pressure Ratio and Discharge System Pressure Ratio.

COMBINING THE PROPELLANT SYSTEMS WITH THE SUPPORTING STRUCTURE

A simplified block diagram to illustrate how the propellant system analysis can be combined with the supporting structure is shown in Figure 10. The fuel and oxidizer injector outflow oscillations as computed above are converted to a thrust oscillation by use of the engine thrust relations. The pump and tank motions which excite the propellant systems are computed from the structure dynamic equations of motion from this known thrust oscillation. From the pump motion the injector outflow oscillation is computed which completes the closed loop self excited system.

To determine the stability of this system the loop can be opened at the input to the structure and a conventional open loop stability analysis can be done. Since the scope of this paper is the analysis of the propellant systems, the stability problem will not be presented in any further detail.

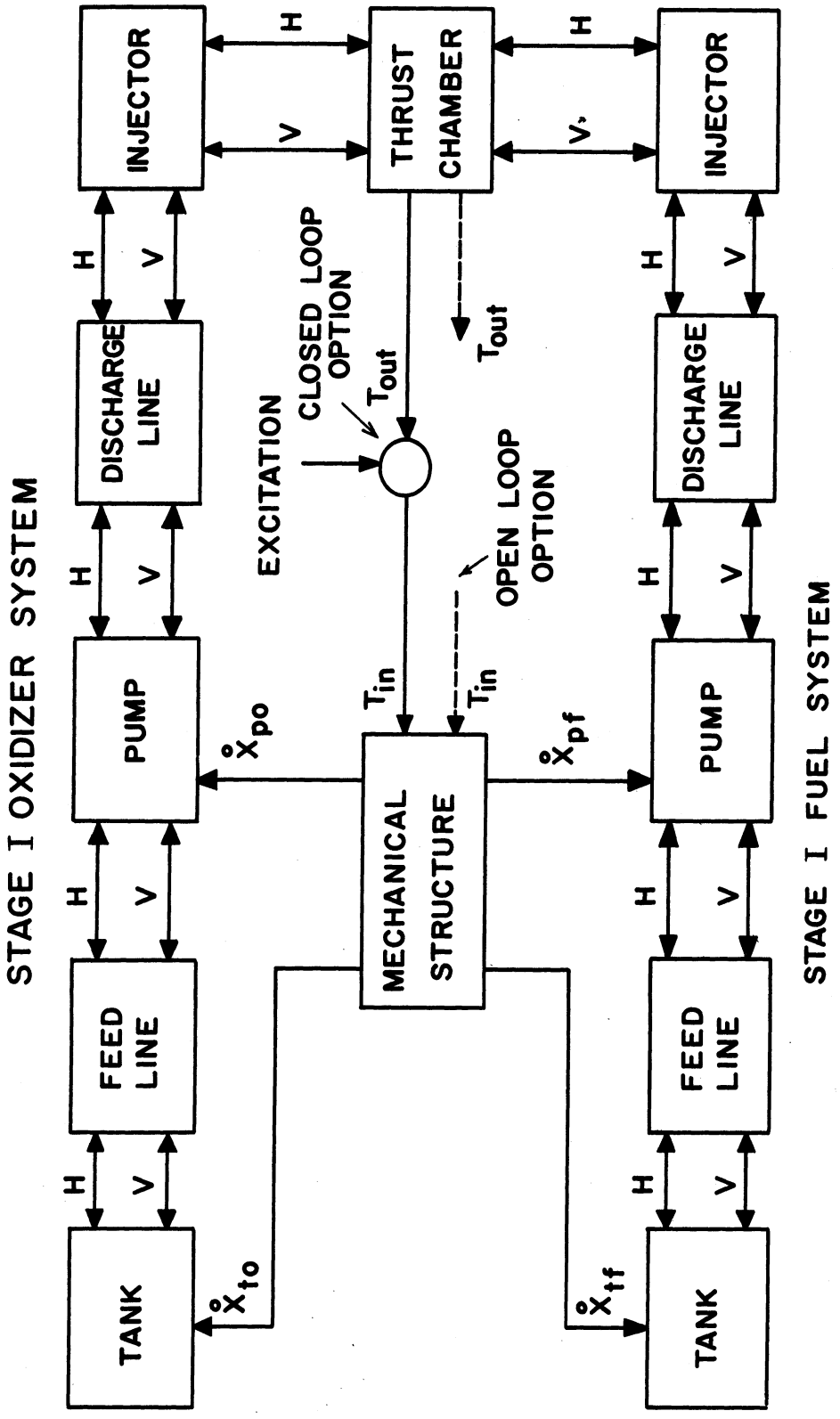

Figure 10. Diagram of Combined Propellant System, Engine, and Structure Analysis.

CONCLUSIONS

The transient flow in a liquid rocket engine propellant feed system including turbopumps can be predicted when the effect of the pump cavitation on the resonant frequency of the system is known. The steady state pump characteristic curves (head rise as functions of flow rate and inlet pressure) were found adequate for the transient problem. The pump transient pressure ratio, defined as the amplitude of the discharge pressure oscillation per unit of inlet pressure oscillation, is predictable.

APPENDIX A

NOTATION

Symbol	Description	Units
a	velocity - pressure wave	ft/sec
b	wall thickness - pipe	ft
B_0, B_1, B_2, B_3	constants - pump curve	
C_{DO}	discharge coefficient - orifice	
C_{DV}	discharge coefficient - venturi	
D	diameter - pipe	ft
D_o	diameter - orifice	ft
D_V	diameter - venturi throat	ft
E	Young's modulus - pipe wall	lb/ft^2
f	Darcy-Weisbach friction coefficient	
f_n	quarter wave resonant frequency	cps
g	gravitation constant	ft/sec^2
H	pressure head	ft
ΔH	pressure head differential	ft
ΔH_{po}	constant - pump curve	
ΔH_p	pressure head rise - pump	ft
H_o	pressure head - orifice discharge	ft
H_g	pressure head - tank gas	ft
H_V	vapor pressure head - fluid	ft
H_{po}	constant - pump curve	ft
$H_p(c,d)$	pressure head, pipe c, section d	ft

K	bulk modulus - fluid	lb/ft^2
L_o	pulser stroke	ft
L_p	pump flow path length	ft
L	pipe length	ft
N1, N2, etc.	number of sections in pipe 1, pipe 2, etc.	
t	time	sec.
Δt	time increment	sec.
V	velocity - fluid	ft/sec
V_o	constant - pump curve	
$V_p(c,d)$	velocity-fluid, pipe c, section d	ft/sec
ΔX	distance increment	ft
Z_o	surge impedance	sec/ft^2
Z	impedance	sec/ft^2
ω	angular frequency - pulser	rad/sec
β	phase velocity	
ρ	mass density - fluid	$slugs/ft^3$
θ	$\Delta t/\Delta X$	sec/ft

Subscripts	Denotes
f	fuel system
O	oxidizer system
1, 2, 3 etc.	pipe number
A, B, C, P	points on characteristics
R, S	interpolated points

REFERENCES

1. "Water-Hammer Analysis Including Fluid Friction", by V. L. Streeter and Chintu Lai, Trans. ASCE, Vol. 128, Part I, (1963), pp. 1491-1552.

2. "Waterhammer Analysis with Nonlinear Frictional Resistance", by V. L. Streeter, Proc. 1st Australâsian Conf. on Hydraulics and Fluid Mechanics, 1962. Pergamon Press, 1963, pp. 431-452.

3. "Waterhammer Analysis of Pipelines", by V. L. Streeter, J. Hyd. Div. Proc. ASCE, paper 3974, (July 1964), pp. 131-172.